 doi:10.20944/preprints202204.0112.v1

Article

A cyanobacteria enriched layer of Shark Bay stromatolites reveals a new *Acaryochloris* strain living in near infrared light

Michael S. Johnson[1*], Brendan P. Burns[2, 3], Andrei Herdean[4], Alexander Angeloski[5], Peter Ralph[4], Therese Morris[3,7], Gareth Kindler[3], Hon Lun Wong[2,7], Unnikrishnan Kuzhiumparambil[4], Lisa M. Sedger[1] and Anthony WD Larkum[4]

[1] School of Life Sciences, University of Technology Sydney, Sydney, Australia.
[2] School of Biotechnology and Biomolecular Sciences, University of New South Wales, Sydney, Australia .
[3] Australian Centre for Astrobiology, University of New South Wales, Sydney, Australia
[4] Climate Change Cluster, University of Technology Sydney, Sydney, Australia.
[5] School of Mathematical and Physical Sciences, University of Technology Sydney, Australia.
[6] School of Earth and Planetary Sciences, Curtin University, Western Australia
[7] Department of Aquatic Microbial Ecology, Institute of Hydrobiology, Biology Centre of the Academy of Sciences of the Czech Republic, České Budějovice, Czech Republic

* Correspondence: Michael.Johnson@uts.edu.au; Tel.: 61 2 0413809670

Abstract: The genus *Acaryochloris* is unique among phototrophic organisms due to the dominance of chlorophyll *d* in its photosynthetic reaction centres and light-harvesting proteins. This allows *Acaryochloris* to capture light energy for photosynthesis over an extended spectrum of up to ~760 nm in the near infra-red (NIR) spectrum. *Acaryochloris sp.* has been reported in a variety of ecological niches, ranging from polar to tropical shallow aquatic sites. Here, we report a new *Acarychloris* strain isolated from an NIR-enriched stratified microbial layer 4-6 mm under the surface of stromatolite mats located in the Hamelin Pool of Shark Bay, Western Australia. Pigment analysis, by traditional spectrometry/fluorometry, flow cytometry and spectral confocal microscopy identify unique patterns in pigment distribution that likely reflect niche adaption. For example, unlike the original *A. marina* species (type strain MBIC11017), this new strain, *Acarychloris LARK001*, shows little change in the chlorophyll *d/a ratio* in response to changes in light wavelength, displays a different Fv/Fm response and lacks detectable levels of phycocyanin. Indeed, 16S rRNA analysis supports the identity of the *A. marina* LARK001 strain as distinct from the *A. marina* HICR111A strain first isolated from Heron Island, previously found on the Great Barrier Reef, under coral rubble on the reef flat. Taken together, *A. marina* LARK001 is a new cyanobacterial strain adapted to the stromatolite matts in Shark Bay.

Keywords: keyword 1; keyword 2; keyword 3 (List three to ten pertinent keywords specific to the article yet reasonably common within the subject discipline.)

1. Introduction

Chlorophyll *d* (Chl *d*)was discovered in 1943 and was first attributed to marine macrophytic red algae [1, 2]. It was the fourth chlorophyll to be discovered, hence the name attribution. It differed from chlorophyll a (Chl *a*) in having a formyl group instead of a divinyl group on Ring 1. This small change meant that the Qy peak was shifted into the infra-red region of the spectrum (peak 720 nm *in vivo*). For the next fifty years the existence of Chl *d* was debated and often relegated to a breakdown product resulting from changes during extraction [3]. More than half a century later, the cyanobacterium *Acaryochloris marina* (strain *Acaryochloris marina* gen. et sp. Nov. [cyanobacteria]) was isolated [4] and later confirmed to be an oxygenic photosynthetic prokaryote containing Chl *d* as its major

 doi:10.20944/preprints202204.0112.v1

photopigment [5]. It was subsequently recognised that the Chl *d* found in red algal species originated from colonial *Acaryochloris* spp. living on the surface of the algae [6-8].

A second isolate was later obtained as a free-living epiphytic cyanobacterium, present on the surface of a number of red algae [8]. Thus, *Acaryochloris* grows as a free-living organism and a large part of the presence of *this species* in didemnid ascidians is due to an epiphytic growth [6, 7]. A third isolate belonging to the *A. marina* clade (strain CCMEE5401) was characterized in 2005, isolated from a unique site at the Salton Sea saltwater lake in California USA [9]. However, a comparison of the 16S rRNA sequences of both strains indicates firstly that they are highly similar (99.2% nucleotide sequence identity) and also that the *A. marina* clade contains a characteristic a small-subunit rRNA gene insertion likely originating from a ◎-proteobacterium; hence *Acaryochloris* is a proteobacterial-cyanobacterial hybrid entity [9].

Several additional strains of *Acaryochloris marina* have been isolated and cultured. *A. marina* MBIC11017 isolated from the squeezed extract of didemnid ascidian in Palau Island (Miyashita et al. 1996, 2003) which is likely the same epiphytic organism also recovered elsewhere [6, 7], *A. marina* AWAJI-1 isolated as an epiphyte from red algae in Japan [8], *A. marina* sp. CCMEE 5410 isolated form eutrophic hypersaline lake, Salton Sea, California (Miller et al. 2005)(Op Cit.), *A. marina* sp HICR111A isolated from dead coral on the reef flat at Heron Island, Australia [10] and the recently isolated strains, *A. marina* MPGRS1 - an epiphyte from red algae *Gelidium caulacantheum* collected from Georges River, Australia [11] and another from a shaded calcified substrate on a coral reef [12]. Of note, *A. marina* has also been found in stromatolites in a number of habitats [13, 14] including Antarctica [15], although 16 S rRNA data is lacking from these more recently isolated strains.

Unlike most other photooxygenic organisms, *A. marina* uses Chl *d*, instead of Chl *a*, as a main pigment in the reaction centres and for photosynthetic light-harvesting. Chl *d*, like Chl *a*, absorbs light in the blue (440 nm) region of the visible spectrum and differs at longer wavelengths by absorbing in the near-infrared (NIR) region (720 nm *in vivo*) - rather than the red region of the visible spectrum. Chl *d* was at first believed to be unique to the genus *Acaryochloris* (Miyashita et al., 2003, 2004). However, Chl *d* has been found in a range of cyanobacteria [16-21], including some cyanobacteria that possess both Chl *d* and Chl *f* [18, 21]. Investigation of the gene cluster FaRLiP (Far Red Light Photoacclimation) indicates this is a genetic loci responsible for the synthesis of Chl *d* and Chl *f* in several cyanobacteria - correlating with the capability of growing in far-red light [18](Op. Cit). In cyanobacterial species containing FaRLiP, Chl *d* forms only a minor part of the total chlorophyll. Nevertheless, all analyses of 16S rRNA sequence data of *A. marina* cyanobacteria from environmental DNA samples, that have been examined to date, indicate that these photosynthetic bacteria are very widespread in nature [22-25]. Despite Chl *d* having been discovered in 2003/2004 in a range of other cyanobacterial genera (op. cit)., it is only recently that a second species, *Acayochloris thomasi*, [26] has been identified. This species differs from all other isolates of *Acaryochloris* in that it completely lacks *Chl d*, but rather has a monovinyl-Chl *a* and *b* content similar to that in *Prochloron* and *Prochlorothrix*.

The genome of *A. marina* MBIC11017 (type strain) which was recently analysed and found to be one of the largest cyanobacterial genomes comprising 8.3 million nucleotides distributed between one master chromosome of 6 503 724 base pairs and 9 plasmids (Swingley et al., 2008). This unusual genome organization, particularly the fact that approximately 25% of its genes reside in plasmids, gave rise to the idea of an increased plasmid-based lateral gene transfer within this genus [27]. Furthermore, the genes located within the plasmid components include those that code for small-molecule biosynthesis, central or intermediary metabolism, energy metabolism, signal transduction, DNA metabolism, transcription, protein synthesis/fate, and surface-associated features [27]. Presumably the plasmids have the capacity for lateral gene transfer to confer an environmental adaptation advantage. Despite these intriguing features of the type strain, the *Acaryochloris* species as a whole, is still poorly described genetically and phenotypically using currently available technologies.

 doi:10.20944/preprints202204.0112.v1

Here, we have characterised a strain of *A. marina* isolated from the 4-6 mm layer of smooth stromatolites from Nilemah, Hamelin Pool of Shark Bay, in Western Australia. This layer receives mainly NIR radiation [28] consistent with the need for specialized NIR absorbing chlorophylls, such as Chl *d* and/or Chl *f*. This study therefore characterises this unique *A. marina* strain from Australian stromatolites and compares it with the *A. marina* type strain (MBIC11017), using 16S phylogenetic typing and pigment analysis by spectrometry/fluorometry, flow cytometry and spectral confocal microscopy, to reveal its unique pattern in pigment distribution that likely reflects stromatolite niche adaption.

2. Materials and Methods

Site description, sampling and mat sectioning

Sampling was undertaken at Nilemah, on the southern shore of Hamelin Pool (26°27′336″S, 114°05.762″E), at 1200h on 21 June 2015 (see Fig 1A). At the time of sampling, the water temperature was 20.1°C, salinity 67.4 PSU (Practical Salinity Units), and pH 8.13. Samples were collected under DBCA license FO25000229-2, and the research was conducted on Malgana country and in consultation with the traditional owners. Mat types analysed here were designated smooth mats, as they are extensively distributed in Shark Bay, and have been examined in detail at the taxonomic and metagenomic levels [29-32]. A map showing the location of sampling is shown Fig 1A. Sections of mat approx. 5 x 5 cm and 2 cm deep were obtained with a sharp knife and placed in waterproof plastic containers for air transport to the University of Technology Sydney within 24h; they were then sored at 4°C in the dark until examination within 2 months. For confocal microscopy thin sections (Fig 1B) of the mat material were obtained and placed on slides which were examined with a Nikon A1 Confocal Microscope equipped with a spectral detection capability. These mat samples are considered representative of stromatolitic mats in Shark Bay, as shown by previous studies. Cultures of *A. marina* MBIC11017 were obtained from the laboratory of Prof Min Chen at the University of Sydney. The specifications for confocal microscopy were set so as to excite fluorescence by NIR chlorophylls: Chl *d* fluorescing at 720 - 740 nm (ex at 458 nm) Chl *f* at 745 - 755 nm (ex at 458 nm).

Isolation and culturing

The overall isolation and culturing strategy is summarised in Figure 1B.

Liquid culture enrichment

Culture aggregates from the 4 – 6 mm layer of several stromatolite samples were ground up in a glass homogeniser and was resuspended in BG11 media supplemented with artificial seawater and incubated in NIR radiation (720 nm, 10 μJ m^{-2} s^{-1}) for up to 12 weeks. Further subculturing involved homogenising 10 mL of the existing culture with a 10 mL *Potter-Elvehjem (glass-teflon)* hand homogeniser, by several strokes and diluting homogenate into new media at 1/10 ratio.

Culturing on agar plates

A 500 μl of aliquot liquid culture homogenate was spread onto agar plates (BG11 supplemented with artificial seawater) and incubated as above in NIR or white light. Single green colonies were selected and re-inoculated with a sterile loop onto BG11 supplemented seawater agar plates and grown in white light (WL), 100 μJ m^{-2} s^{-1}) or NIR radiation (720 nm, 10 μJ m^{-2} s^{-1}) for up to 12 weeks (Fig. 1B).

Preprints (www.preprints.org) | NOT PEER-REVIEWED | Posted: 12 April 2022 doi:10.20944/preprints202204.0112.v1

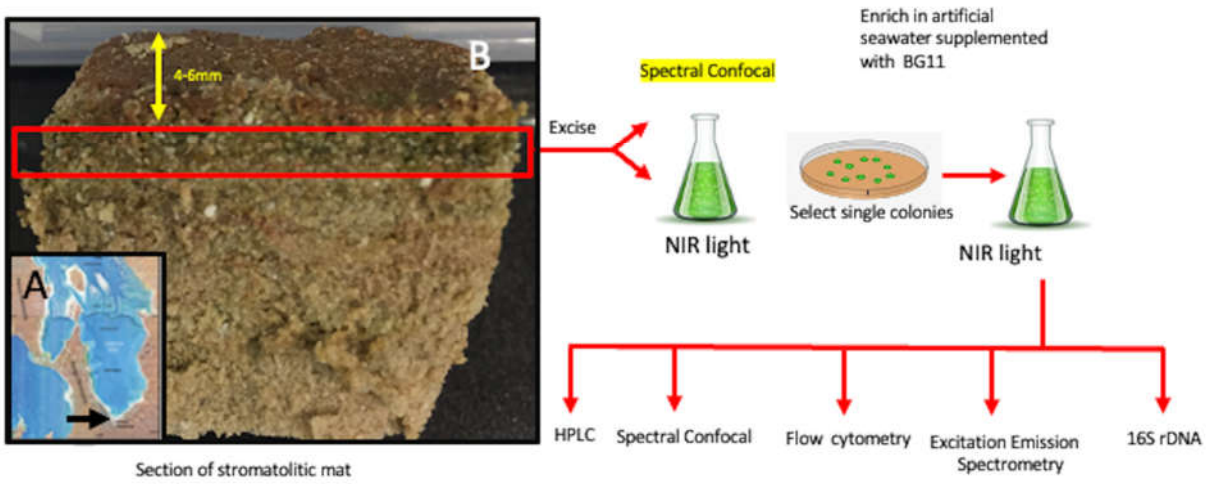

Figure 1. Sampling and enrichment: (a) Map showing Hamelin Pool, with an arrow indicating the position of the sampling site at Nilemah. (b) Overview of sampling, culture enrichment and analysis methods.

Fluorescence microscopy:

Hyperspectral confocal microscopy was used to determine emission spectra matched to cell morphologies. Mat samples sections, small aliquots of liquid culture or colonies from agar plates were laid onto WPI Fluoro-dishes (coverslip thickness 0.017mm) and images scanned on a Nikon A1 Confocal microscope using the 458nm laser with emission collected through the spectral detector, in order to obtain a lambda stack. Cells of interest were highlighted by Regions of Interest (ROIs) and emission spectra collected for those cells.

For 3D imaging of isolates from liquid culture, cells were fixed in 4% Paraformaldehyde/PBS and mounted on a 0.017mm coverslip in prolong glass (NA1.520) mounting medium (Thermo) and imaged on a Leica Stellaris 8 Confocal microscope with a 63X oil object (NA1.4). Excitation and emission settings were set to detect phycocyanin fluorescence (ex 620nm, em 675/10nm) and Chl *d* fluorescence (excitation 708nm, emission 720/10nm). A step size of 100nm was used to collect the whole volume of the cells. For morphometric analysis, the fixed and mounted cells (above) were imaged on an Olympus BX51 epifluorescence microscope fitted with a 100X oil immersion objective (NA1.3) and an Olympus DP73 camera. Both brightfield and fluorescence images (excitation 530nm-500nm emission 575nm LP) were collected. Cell shape (aspect ratio) and size (diameter) were determined by using Image J - FIJI [33]. For each isolate, a threshold level was set for the red auto-fluorescence where the fluorescence perimeter of the cells to matched the brightfield perimeter. The segmented cells were made into a binary image and any joining cells were separated by water-shedding. The analyze particle function was then used to determine the shape (aspect ratio). Further segmentation based on circularity (where non-round/elongated cells ie with circularity less than 0.8 were discarded) was applied and the diameter of these "round" cells was also determined using the analyze particle function.

Absorbance and fluorescence spectroscopy

 doi:10.20944/preprints202204.0112.v1

Slides of cultured *Acaryochloris sp.* were placed on glass microscope slides with coverslips and placed on a upright microscope stage (Nikon Ti) with a 40X (NA0.6) objective at room temperature. The cells were brought into the focal plane under white light. The light that passed through the cells was measured with a spectrometer (Avantes Avaspec with a spectral resolution of 0.4nm) connected via an optical cable to one of the oculars of the microscope. An area devoid of cells was used to collect the background spectra, that was later subtracted in the image analysis processing.

Excitation emission matrices

Liquid cultures were placed into the wells of a 96 welled (black walled) plate and the fluorescence emissions at every wavelength from 620-760nm were measured at every excitation wavelength from 300 – 750 nm in a fluorescence plate reader (Tecan Infinite M1000 Pro). Raw data was exported to Microsoft Excel and heatmaps were created as described by [34].

HPLC Pigment analysis

High performance liquid chromatography (HPLC) was used to determine concentrations Chl *a* and *d* in the *Acaryochloris* cultures gown in either white light or NIR cultures. One hundred mL of each culture was pelleted at 10000g for 10 minutes to collect the biomass for pigment signal detection. Extraction of samples were carried out following [35] with slight modifications. Chilled acetone was added to the pelleted biomass, sonicated (30 s at 50W) and then vortexed three times for 30 s each under cold, dark conditions to limit pigment degradation, and then stored at 4°C overnight. Pigment extracts were then filtered through a 0.2 µM PTFE 13 mm syringe filter and stored in -80°C until analysis. An Agilent 1290 HPLC system equipped with a binary pump with integrated vacuum degasser, thermostat controlled column compartment modules, Infinity 1290 autosampler and PDA detector was used for the analysis. Column separation was performed using an Agilent's Zorbax Eclipse C18 HPLC 4.6 mm × 150 mm column using a gradient of ammonium acetate (0.01M), methanol, acetonitrile and ethyl acetate as per a previously reported method (1 (method C). A sandwich injection approach was set using the auto injector program, where the mixture of MeOH: ACN (8:2) and samples were drawn alternatively in the sequence, 100: 60: 100 (µL) and then mixed in the loop and injected (this is the modified part of the method). A complete pigment spectrum from 270 to 780 nm was recorded using PDA detector with 3.4 nm bandwidth. Following wavelengths were used to monitor the chromatogram: 406, 696, 706 nm, 440 and 660 nm

16S rRNA analysis.

DNA was extracted using the DNeasy PowerBiofilm Kit DNA extraction kit (QIAGEN) according to the manufacturer's instructions. Biological duplicates were extracted separately then pooled prior to sequencing to minimise potential heterogeneity biases. Purified DNA samples were sequenced on an Illumina MiSeq for 16S V1-V3 amplicon (27F-519R) on a v3 2x300 bp run by the Ramaciotti Centre for Genomics (UNSW Sydney, Australia). Sequences were processed through the Mothur pipeline [36] with default parameters, with searches of representative sequences against the SILVA [37] database. For the most abundant sequence in the cultures, representative sequences were then aligned against Cyanobacteria 16S rRNA sequences retrieved from the SILVA and NCBI databases [38], with Chloroflexi as the outgroup. A maximum likelihood tree was constructed with IQ-TREE2 with 1000 bootstraps [39] and visualized using iTOL [40]

Flow cytometry.

Sample acquisition and instrument settings. Cyanobacterial broth liquid cultures (5 mL aliquots) were prepared for flow cytometry analysis by executing 5 strokes of a *Potter-Elvehjem (glass-teflon)* hand homogenizer tube to break up any cell culture clumps and bacterial aggregates. Cyanobacterial cell cultures were run on an LSRII flow cytometer (Becton Dickenson, BD Biosciences) with DIVA acquisition software (version 8.0.2). First,

 doi:10.20944/preprints202204.0112.v1

FSC-A/SSC-A two-parameter dot plots were viewed with logarithmic scale settings. First, sterile normal saline was acquired for 1 min pre-cyanobacterial sample acquisition. This permitted detection of electronic noise events and permitted subsequent gating on larger events of cyanobacteria (R1) from the liquid cultures. Next, cell events were collected for each culture sample, before again running sterile saline also for 1 min. Voltages were set such that electronic noise and any non-fluorescent cyanobacterial were located in the bottom left-hand panel of two-parameter dot plots of all fluorescence detection channels. Thus, natural fluorescence was evident as events with higher laser-excited fluorescent emission, without any staining. Data were saved and exported as FCS3 data files.

Cytometry Data Analysis. Samples file events were set to the same minimum 80,000 number using the DownsizeSampleV3 plugin. Samples were first viewed as two-parameter FSC-A/SSC-A dotplots. Uncompensated data was also concatenated for subsequent analysis for SSC-A distribution (or FSC-A distribution) versus sample ID to confirm cyanobacterial events (R1) as distinct from electronic noise events (*). Events in R1 were assessed as FSC-A data via histogram overlays - gating on very small cells and debris, small cells, and large cells. Uncompensated two-parameter fluorescence data excited by the 640nm red laser were chosen for the fluorescent analysis, as this represented the presence or abundance of phycocyanin (detected via the 660/20nm bandpass filter in detector array position C) and Chl *d* (detected via the 730/45nm bandpass filter in detector array position B). All cytometry analysis and data overlays were performed with FlowJo (version 10.8.1) and multi-component data figures prepared in Microsoft Powerpoint for Mac (version 16.57).

Fluorometry by Pulsed Amplitude Modulated (PAM) fluorescence

Quantum yield of photosystem II (F_v/F_m) was determined the MAXI PAM model IMAG-MAX/L (Walz, Effeltrich, Germany) fluorometer. The instrument was fitted with blue actinic light emitting diodes (LEDs) with a peak wavelength of 450 nm that were used for applying the saturation pulse for determination of F_m, and for determination of F_o. Samples were dark adapted for 10 minutes prior to the measurement. After image acquisition and data processing was performed with the ImagingWin v2.56p instrument software. [41]

3. Results

This section may be divided by subheadings. It should provide a concise and precise description of the experimental results, their interpretation, as well as the experimental conclusions that can be drawn.

3.1. Location

Cyanobacteria were isolated from stromatolite mats located at Nilemah in Hamelin pool (Figure 1A). This is an area of high salinity due to the isolation of the Hamelin pool from the rest of Shark Bay, due to a sill at the entrance to the Hamelin Pool (salinity 66-72 PSU Location 26.1667° S, 114.0833° E). A sample was collected and transported to UTS for the various analysis. It was stored at 4°C in the dark prior to analysis.

3.2. Confocal Imaging of mat material

Hyperspectral confocal images were obtained of the mat at 4 – 6 mm from the upper surface. Both coccoid and filamentous cyanobacterial cells were visualised. Emission wavelengths evident from the filamentous cells exhibited a peak at 745 -750 nm in indicating Chl *f* (Figure 2A) and coccoid cells with a peak at approximately 735nm indicating Chl *d* (Figure 2B). The filamentous cells with the 745 – 750 nm peak emission also had a significant peak in the red at 680-685 nm indicating the presence of significant amounts of Chl *a* (Figure 2A). There were also coccoid cells with spectral emission profile indicative of mainly Chl *a* (Fig.2A – data not shown). Hyperspectral confocal

 doi:10.20944/preprints202204.0112.v1

imaging of an initial culture enrichment in NIR, indicated the presence of coccoid cells with an emission peak of 735nm, filamentous cells with an emission peak of 728nm and diatoms with an emission peak of 710nm (Fig 2C)

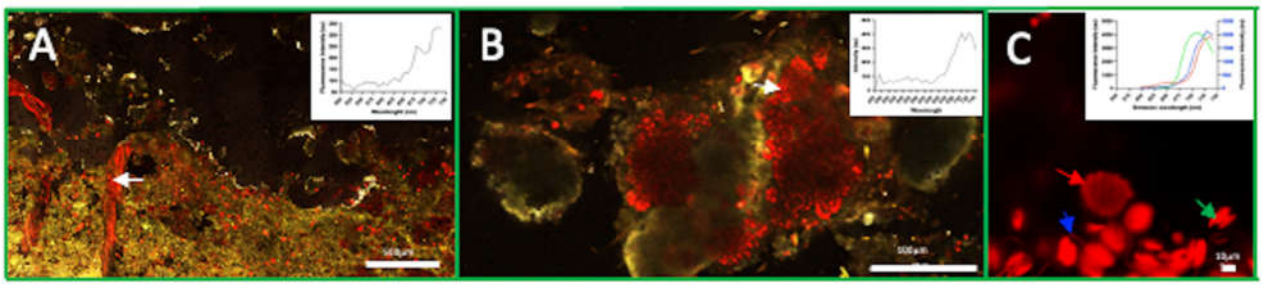

Figure 2. Confocal Imaging of green layer. A side view of an excised segment randomly sampled from a smooth mat at Nilemah. (a) A large section (1cm x 0.6 cm) of the green layer imaged by hyperspectral confocal microscopy using a 458 nm laser with 10nm continuous band pass emissions collected up to 750nm. The red organisms consist of red and far red/NIR (700-750nm) fluorescing pigments. Both filamentous and coccoid forms are observed. The filamentous forms (white arrow) contain a far-red emitting (750nm peak) pigment that is most likely Chl *f*. (b) Emission spectra of typical coccoid cell (yellow arrow) when excited by the 458 nm laser. 2 peaks are evident at 704 nm and 724 nm, suggestive of the presence of Chl *d* (724nm). (c) Arrow shows the various microbial forms that were found in the initial NIR enrichment culture. The green arrow shows a diatom (emission peak 710nm), the blue arrow shows a filamentous form (emission peak 730 nm) and the green arrow shows a cluster of coccoid cells (emission peak 730nm).

3.3. Obtaining a purified isolate and culture morphology

Sub-sampling of the enriched culture resulted in the growth of the coccoid forms as colonies on agar plates in NIR. Further subculturing of agar plates in NIR of single colonies led to the isolation of a single colonies on agar plates (Figure S1 Panel B) The MBIC11017 type strain had a propensity to form large clusters, compared with LARK001 strain, when grown in liquid culture in NIR (Fig S1, panel A). The LARK001 strain exhibited a yellow green colour when grown on agar or when grown in liquid culture, whereas the MBIC11017 strain exhibited a darker blue green colour in the same conditions.

3.4. HPLC analysis

HPLC analysis revealed that both the LARK001 strain and MBIC11017 strain possess Chlorohyll *d* as their major photosynthetic pigment. The chl *d* content in the LARK001 strain remained consistent in response to light condition, with chl *d* making up 93.4% of chlorophyll content in white light and 92.9% in NIR (Table S1). However, the MBIC11017 strain showed a marked difference in chlorophyll content in response to light conditions, with a 91% chl *d* content evident in cells grown in white light that increased to 96.4% chll *d* in cells grown in NIR (Table S1).

Preprints (www.preprints.org) | NOT PEER-REVIEWED | Posted: 12 April 2022 doi:10.20944/preprints202204.0112.v1

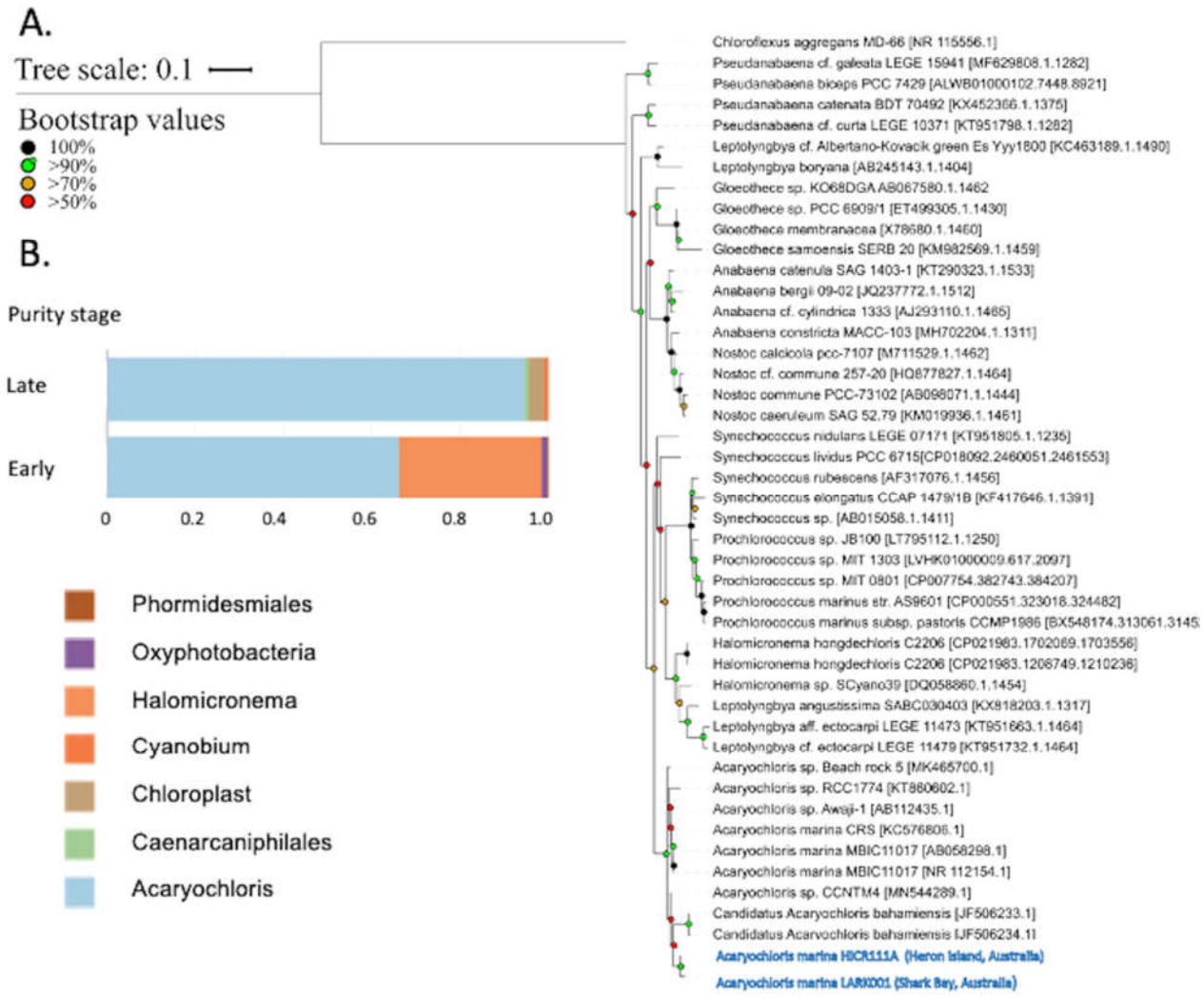

Figure 3 16S rRNA sequencing. (a) 16S rRNA gene phylogeny of the LARK001 isolate from showing the relationship to other isolates. (b) 16S rRNA gene sequence representation of the LARK001 isolate at different stages of culture purification.

3.5. Sequence Identity

The 16S DNA sequence identity of cultured cyanobacterial from Shark Bay stromatolites, *A. marina* LARK001 indicated that is forms a clade closely linked to *A. marina* HICR111A first isolated from Heron Island, as demonstrated by maximum likelihood phylogenetic tree analyses of representative species (Figure 3A). Indeed, whilst the LARK001 isolate is clearly an *A. marina* cyanobacteria, it clusters away from the *A. marina* MBIC11017 type strain (Figure 3A). Moreover, although not entirely genetically pure, this LARK001 in vitro cultured isolate is over 95% *A. marina* and can sustain in vitro growth as isolated together in co-culture with up to 3 other species (Figure 3B). In the initial enrichment, 16S rRNA analysis indicated the presence *Phormidesmiales, Oxyphotobacteria, Halomicronema* along with *Acaryochloris*. In the late enriched culture a 16S rRNA gene analysis revealed the presence *Halomicronema* and Chloroplasts (most likely diatoms) which were both also found by confocal microscopy in an enriched culture – see Figure 2C. It is interesting to see the presence *Caenarcaniphilales* in the late enriched culture.

 doi:10.20944/preprints202204.0112.v1

These are a newly described order of organisms, belonging to the phylum Melainabacteria, that share phylogenetic and structural similarities with cyanobacteria, but lack the ability to photosynthesise. Nevertheless, this new Australian *Acaryochloris* strain, constituted 95% of the late enriched culture and is distinctly phylogenetically distant from the clade containing the MBIC11017 type strain

3.6. Spectroscopic analysis

Next an absorbance spectral analysis was performed on cultures of the *A. marina* MBIC11017 strain and *A. marina* LARK001 strain. The absorbance peak of *A. marina* MBIC11017 was 710nm, whereas that of *A. marina* LARK0001 was at 704nm (Figure 4B). However, whilst *A. marina* MBIC11017 has in addition a distinct absorbance peak at 610-640 nm (attributed to phycocyanin), this was not detectable in the new *A. marina* LARK001 (Figure 4A). The fluorescence emission spectra of the two strains differed markedly (Figure 4C): *A marina* MBIC11017 had a major emission peak at ~724 nm, whereas the *A. marina* LARK001 had a major peak at 735nm (Figure 4C). Excitation emission scanning further highlighted the different profiles of these strain (Figure 4D). Notably, an additional fluorescence emission peak at 650nm (attributed to phycocyanin) is present in the A. marina MBIC11017 strain and is not present in LARK001 (Figure 4C). Finally, spectral confocal imaging analysis also confirmed Chl *d* fluorescence emission peaks of 715nm were evident for the *A. marina* MBIC11017, but in *A. marina* LARK001 (Figure 4D; panels E-F) an additional fluorescence emission peak of 735nm appears to predominate. Despite differences in the spectral characteristic at a cellular *in vivo* level, there were no such differences observed in the absorbance profiles in the HPLC chl *d* fraction from each strain (Panel F).

3.7. Flow cytometry and morphometric analysis

In vitro cultures of *A. marina* MBIC11017 and LARK001 were examined by flow cytometry, after homogenisation to enable single cell cytometry. The small size and diverse culture shapes of these cyanobacteria are evident in forward and side scatter dotplots, and the preparation procedure appears to produce very small cells and debris, but these are easily made distinct from electronic noise by comparing files generated by saline (without cyanobacteria) and gating on side-scatter, or forward scatter profiles (Figure 5A). Thus, the in vitro cultured cyanobacteria cells were detected in three general size groupings: very small, small and large (Figure 5A). Simple two-parameter uncompensated fluorescent data overlays of 640 nm red-laser excited emission profiles can easily profile both phycocyanin (evident on the 660/20nm bandpass / detector channel) and Chl d (detected at 730/45nm detector channel), where distinct populations are evident (Figure 5B). A clear feature of this data is that the largest cells contain the most abundant Chl d, and the presence of phycocyanin in MBIC11017 type strain easily separates the two strains (Figure 5C). In comparison the small cells both contain low fluorescence in 660/20nm and 7300/45nm, and the very small cells and debris are either weakly or non-fluorescent in these channels (Figure 5C). The flow cytometry profiles also closely mirrored images of two strains, obtained by confocal fluorescent microscopy (Figure 5D), using the 620nm laser excitation and collecting emissions 675/10nm for phycocyanin fluorescence and laser excitation at 708nm with emissions collected at 720/10 nm for Chl *d* (Figure 5D). Here, 3D rendering indicated that, in the MBIC11017 strain the phyocyanin was present near the periphery of the cells and Chl d situated throughout the entire cell volume (Figure 5D), whereas no phycocyanin was present in the LARK001 strain.

 doi:10.20944/preprints202204.0112.v1

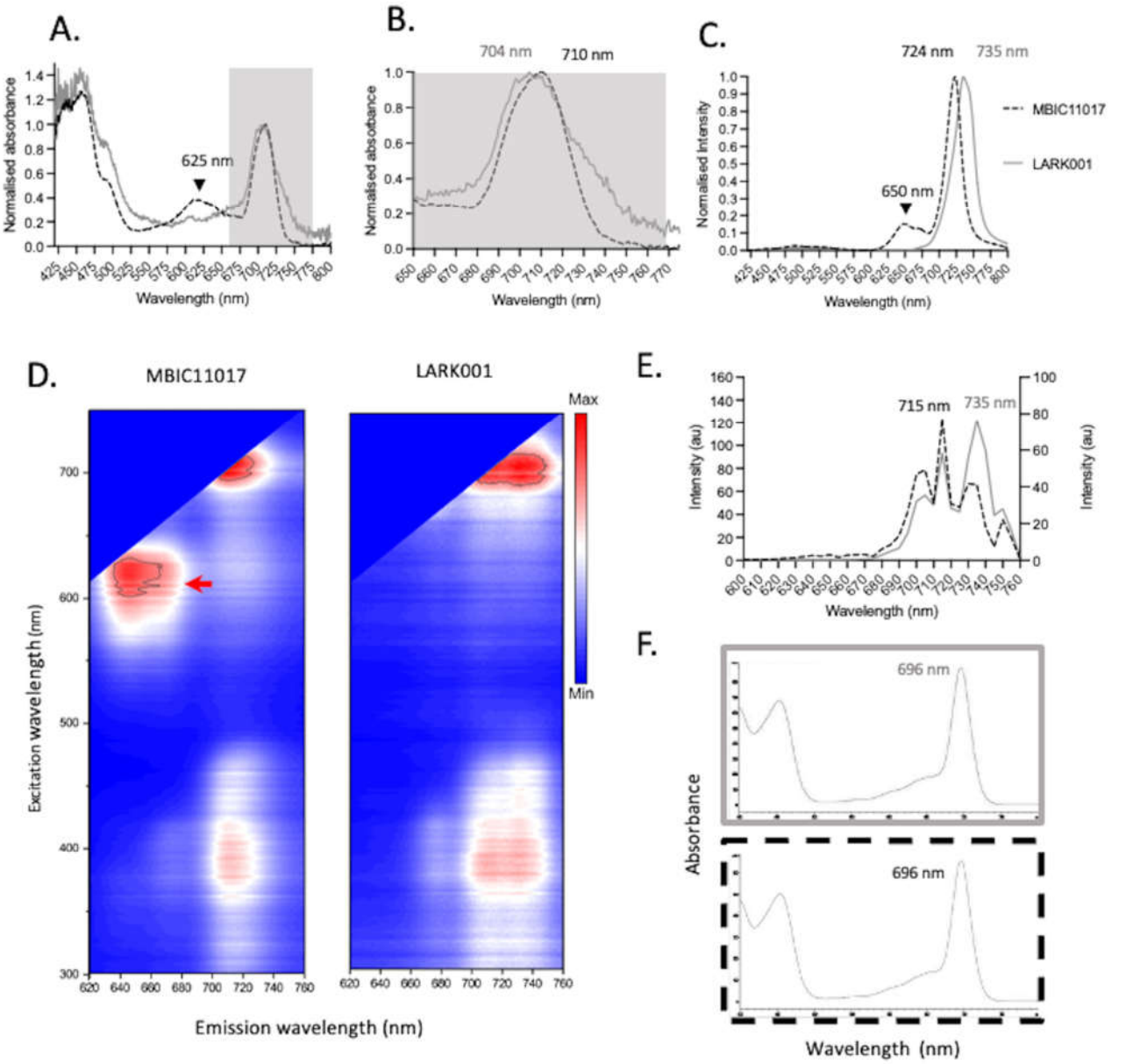

Figure 4. Absorbance spectra and fluorescence spectra of *A. marina* MBIC11017 vs *A. marina* grown in NIR. (a) Absorption spectra of both strains indicates differences between the two stains At 625 nm (black arrow) a peak is present in the MBIC11017 strain that is not present in the LARK001 strain. Differences in the Chl *d* absorption region are also present (grey boxed region). (b) The grey boxed region from Panel A is magnified to further highlight the difference in peak Chl *d* absorption from 704nm for LARK001 and 710nm for MBIC11017. (c) The emission profile for each strain, reveals a peak at 650nm (black arrow) that is unique in the MBIC11017 strain, whilst the Chl *d* emission peaks differs substantially with the peaks at 724nm and 735nm for MBIC11017 and 735nm for LARK001 strain. (d) An excitation emission matrix shows a unique spectral component (ex max approx. 625nm and em max approx. 640nm) in the MBIC11017 strain. The LARK001 strain exhibits 2 distinct emission profiles at for Chl *d* at 718nm (approx.) and 735nm (approx). Only one emission profile at 718nm approx. is evident for the MBIC11017 strain. (e). Hyperspectral confocal scan (top panel) confirms the evidence of two emission peaks in LARK001, with the 735 nm peak the major contributor in this strain. The same two peaks are evident in the MBIC11017 strain, but the 715 nm peak is the major peak. (f)The grey and black dashed panels reveal no difference absorbance profiles in the Chl *d* fraction that was purified by HPLC for each strain.

Preprints (www.preprints.org) | NOT PEER-REVIEWED | Posted: 12 April 2022 doi:10.20944/preprints202204.0112.v1

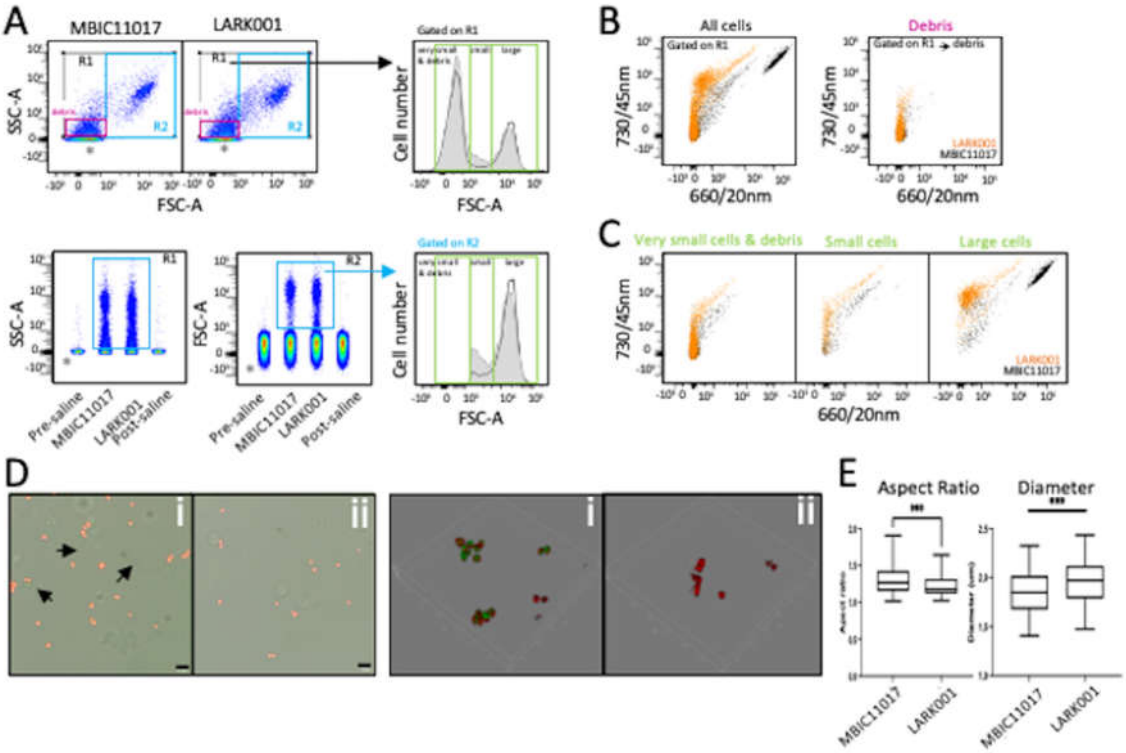

Figure 5. Cytometry and confocal microscopy analysis of A. *marina* type strains MBIC11017 and LARK001. (a) MBIC11017 and LARK001 cyanobacterial cells in FSC-A/SSC-A dotplots indicating distinct cell populations. Also shown are concatenated SSC-A distribution data, confirming electronic noise events in pre- and post-saline samples (acquired for 1 min). Cell events in R1 exclude electronic noise (*) and demonstrate evidence of two sub-populations based on cell size: designated smaller (R2) and larger (R3) cyanobacteria cells in histogram overlays: MBIC11017 (black unfilled histogram) and LARK001 (grey filled histogram). Tiny debris events are also evident within the R1 gate, but size gating (R4) removes these events. Arrow indicate the shoulder of slightly larger cells within the R2 gated population. (b) Two-parameter dot plots of natural fluorescence at 730/45 nm versus 660/20 nm in *A. marina* MBIC11017 (black) and LARK001 (orange) strains upon 640nm red laser excitation. (c) Two-parameter dotplots of fluorescence at 730/45 nm versus FSC-A for R2 and R3 gated events of *A. marina* MBIC11017 (black) and LARK001 (orange) strains, also upon 640nm red laser excitation. (d) Confocal images of (i) *A. marina* MBIC11017 (i) and *A. marina* LARK001 (ii) cells (scale bar is 5mm), also shown are 3-D rendered images of the same two strains. (e) Aspect-ratio (n=107 for MBIC11017 and n=94 for LARK001) and diameter analysis (n= 65 for MBIC11017 and n=73 for LARK001) of cells from microscopy data acquired in D. *** P<0.005 by student t-test.

Finally, both the cytometry side scatter profiles and confocal imaging strongly suggested that the MBIC11017 strain and the LARK001 may exhibit morphometry differences. Therefore, the fluorescence microscopy image data were analysed with to aspect ratio and diameter, and here, the literal physical shape differences were confirmed to be statistically evident (Figure 5E).

3.8. Fluorometry

Pulse amplitude modulated (PAM) fluorescence measurements facilitated determination of the ratio of variable fluorescence (F_v) to maximum fluorescence (F_m) and hence the potential quantum efficiency of photosystem II for each strain under the each light condition. The F_v/F_m values of the MBIC110117 strain did not appear to change significantly in response to the light condition. However, the LARK001 strain showed a significantly drop in potential quantum efficiency in photosystem II when incubated in

 doi:10.20944/preprints202204.0112.v1

NIR as compared to cells grown in white light (Figure 6 Panel A and B). The LARK0001 cells grown in NIR showed the lowest potential quantum efficiency (F_v/F_m) of the all strain/conditions tested and this was shown to be significantly different from all other strain and conditions combinations tested. Also, the LARK001 strain grown in NIR resulted in the slowest growth conditions, with a 53 day dividing time (Figure 6 Panel C). This is more than double the doubling time of any other combination of strain and light condition.

4. Discussion

We have isolated a new strain of *A. marina* from stromatolitic mats from the southern end of Hamelin Pool, Shark Bay, in Western Australia. This site is the one designated as available for research in the stromatolite area of the World Heritage Area. It is, in fact, the same site where all approved stromatolite research has been conducted over the >20 years. All of the published and unpublished research, to date, indicate that these structures represent a typical community as found on the columnar stromatolites 20 km East, further along the southern side of the Hamelin pool.

The new Australian stromatolite-derived *A. marina* strain described here (*A. marina* LARK001) differs in several ways from the classic MBIC11017 type strain specie. Firstly, in 16S rRNA phylogenetic analysis the new strain is closest to a previously isolated strain *A. marina* HICR111A [10], from a shallow site on the reef flat at Heron Island, Southern Great Barrier Reef. Consistent with this genetic closeness, the *A. marina* LARK001 has a room-temperature (RT) fluorescence peak at 735nm indicating the abundance of Chl d. Indeed, both HICR111A and LARK001 strains appear to possess in Chl d that is typically conjugated with a specialized pigment proteins that shifts the fluorescence emission to the 735 nm and above. Instead, the MBIC11017 type strain has a shorter RT fluorescence emission ~720 nm indicating that Chl d is the major chlorophyll in both photosystem I and photosystem II and that its light-harvesting chlorophyll protein complex has a fluorescence emission at ~720nm. Thus, it is likely that *A. marina* HICR111A and LARK001 contain a different light-harvesting chl d-binding proteins that causes a shifted emission at 735nm and above at RT. Moreover, the light harvesting chl pigment harvests NIR light efficiently and passes it onto the photosystem II and possibly to photosystem I as well, as evident in the PAM analysis. This interpretation is consistent with HPLC analysis that confirmed only Chl d as the major pigment present within LARK001 cultures; with only a minor amount of Chl a (6-7%) being detected in this analysis (Table S1). Other similarities between HICR111A and LARK001 strains of cyanobacteria is that they both appear to contain very little phycocyanin. Interestingly, LARK001 divides slowly in NIR compared to white light (Figure 6C). On face value we conclude that the two strains of *A. marina* LARK001 and HICR111A have different light harvesting properties compared to the MBIC11017 type strain. This is despite HICR111A occurring on a coral reef in a shaded rubble zone on the reef flat in Eastern Australia, and LARK001 existing several millimeters below the surface of a stromatolitic mat in Hamelin Pool, Western Australia – some 3800 km distant. Both sites are subtropical with respect to latitude (Heron Island 22°S and Hamelin Pool, Shark Bay 26°S) but are differentiated in terms of the ecosystems involved. However, the *A. marina* MBIC11017 type strain was isolated from a tropical sites (Palau 7.5°N) in the western pacific which has a very different ecologically niche to the location we isolated *A. marina* LARK001. Interestingly, Hamelin Pool in Western Australia, Heron Island and Palau are equidistant from each other. However, the *A. marina* MBIC11017 type strain grows much better in NIR light, compared to LARK001. In natural light, the MBIC11017 strain is augmented by some orange-red light (600-700 nm) absorbed by phycocyanin. In this regard the MBIC11017 strain grows on the underside of didemnid ascidians where it

Preprints (www.preprints.org) | NOT PEER-REVIEWED | Posted: 12 April 2022 doi:10.20944/preprints202204.0112.v1

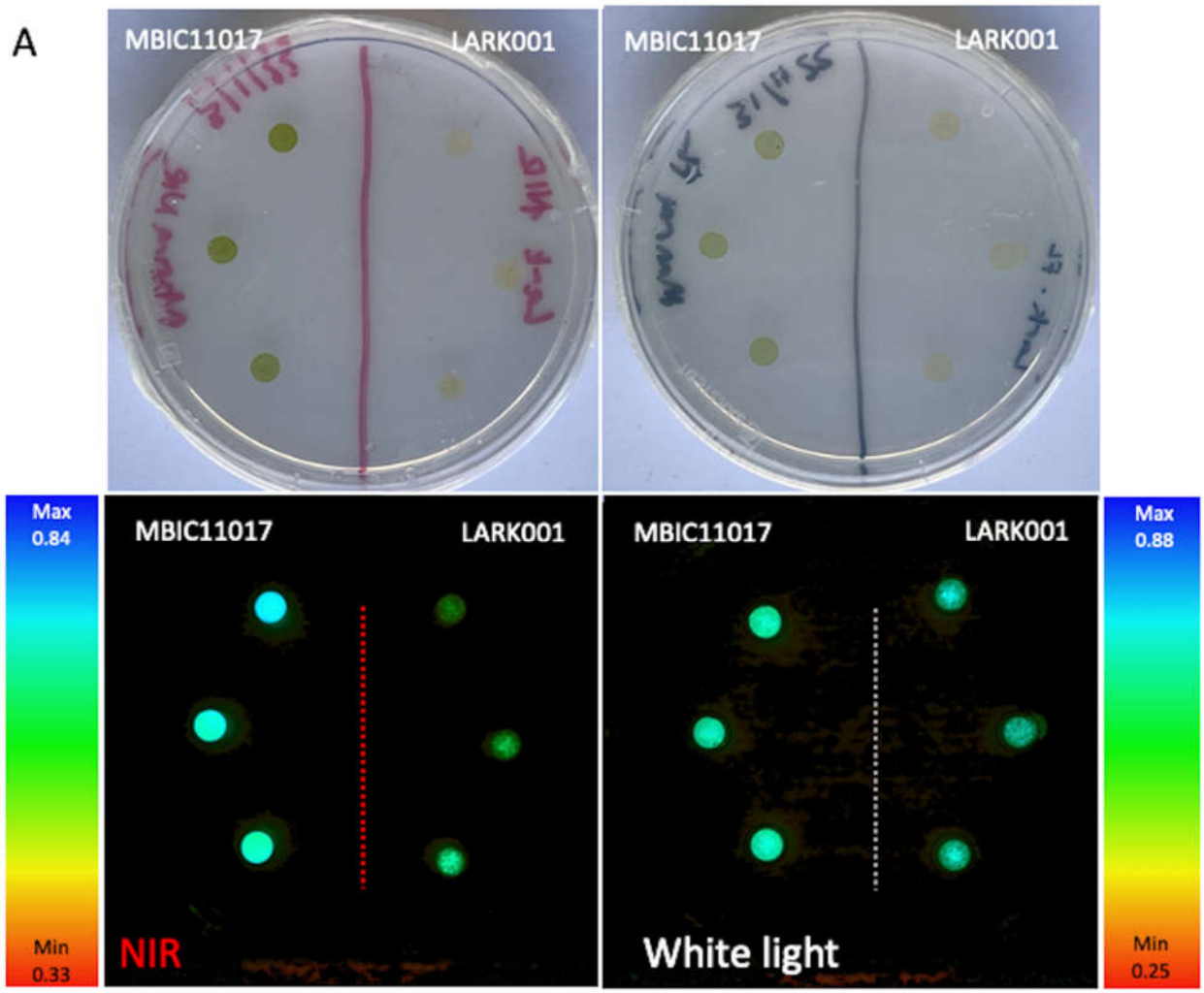

B

STRAIN	MBIC11017		LARK001	
LIGHT CONDITION	NIR	WHITE LIGHT	NIR	WHITE LIGHT
F_v/F_M (n=3)	0.535±0.025	0.491±0.006	0.370±0.066	0.477±0.003

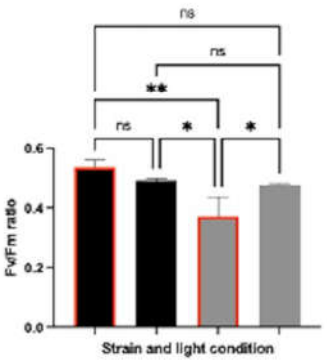

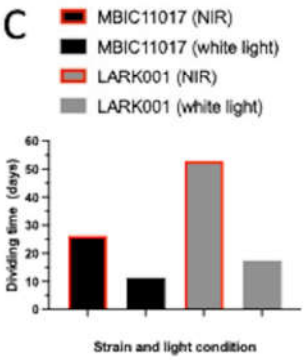

Figure 6. Fluorimetry measurement by PAM. (a) clockwise from top left. Cultures grown for 3 weeks in NIR after a 50,000/25µl cells of each strain were added to the surface of the agar plate in triplicate. Cultures grown for 3 weeks in white light after a 50,000/25µl cells of each strain were added to the surface of the agar plate in triplicate. PAM imaging of the white light incubated cultures. PAM imaging of the NIR incubated cultures. (b) Fv/Fm measurements for the cultures and graph showing pairwise comparison * $p<0.05$, ** $p<0.01$. (c) Doubling time of each strain in either white light or NIR conditions

 doi:10.20944/preprints202204.0112.v1

receives mainly radiation that has been highly filtered by the *Prochloron didemni* that lives in the atrial cavity of the ascidians. Thus, it may generally receive NIR light in the 720 nm range with incidental flecks of light in the orange red spectral region. In contrast both strains *A. marina* LARK001 and HICR111A seem to rely on NIR at 704 -706nm, but also have the ability to exist in white light where Chl *d* can absorb light in the blue region augmented by absorption by the carotenoids (460-540 nm) without any reliance on the phycobiliprotein or phycocyanin, in the orange-red region of the visible spectrum. It remains possible that all *Acaryochloris* strains might also rely on absorption of light by Chl a which is present in all strains, even if in smaller quantities (Table S1).

Present in the confocal microscopy analysis of the mat material were several other bacteria: some with near far-red shifted peaks in their chlorophylls (data not shown). The most abundant of these was what we identified as *Chroococcidiopsis sp*., which possesses Chl f with a fluorescence emission peak at ~750 nm at RT. This *Chroococcidiopsis sp*., has not been previously reported to have been isolated to purity in in vitro culture. Similarly, another cyanobacterium with an apparent red-shifted chlorophyll is *Spirulina sp*., which also has not been isolated to purity to date. Moreover, the 16S genotype sequence data confirm the presence of both of these microorganisms in stromatolite material [23]. Furthermore, the 16S data presented here indicates the presence of other phototrophic bacteria, *Phormidia*, *Halomicronema* and *Cyanobium*, all of which have been detected microscopically (data not shown). Microalgae (chloroplast) are also evident in the 16S data and these were evident microscopically in our initial enriched cultures (Figure 2C). The presence of *Caenarcaniphilales* (malainabacteria) is also of interest. The Melainabacteria are a newly described, non-photosynthetic sister phylum to the Cyanobacteria. They are often found in aphotic environments such as human and animal guts, grassland soil and wastewater treatments [42], and it is interesting that they have been detected in the attenuated light conditions associated with the 4-6mm deep layer studies here.

A subtle but important feature of our data was that both flow cytometry and fluorescence microscopy (with morphometric analysis) demonstrated that the smaller cells within the in vitro culture of *A. marina* LARK001 strain are slightly larger (1.48μm-2.43 μm diameter) than the smaller cells in the MBIC111017 type strain cultures (1.41-2.32 μm diameter). This is in contrast to reports of the size of the HICR111A Heron Island strain which, although also lacking in phycocyanin is a much smaller at 0.75 – 1.00 μm [23]. Hence the 16S genotyping similarities of *A. marina* LARK001 strain to HICR111A also coincide with similarities in its morphometric features – despite the obvious ecological niche significant differences described above. A deeper, full genome analysis of *A. marina* LARK001 is underway in our laboratory, that should better explain and define the similarities and differences between these three strains. This will provide a deeper understanding of genetic limitations and molecular signatures of adaptation capability, and particularly to potential for serious sensitivities of habitat changes within the stromatolite microbial communities, i.e. that would be expected to occur with ongoing climate change impacts, or insults from viral and other microbial predators.

5. Conclusions

We provide here the first physical and initial genetic characterisation of a unique strain of *A. marina* cyanobacteria, termed the LARK001, isolated from ancient Australian stromatolites in Shark Bay, in Western Australia. Using HPLC, spectroscopy, flow cytometry and microscopic techniques, we demonstrate that *A. marina* LARK001 contains plentiful amounts of Chl *d*, minor signatures of Chl *a*, and lacks the phycocyanins that are present in the *A. marina* type strain MBIC11017. Despite

the difference in ecological niches, and large location distance, the *A. marina* LARK001 closest genetic relative is *A. marina* HICR111A strain from Heron Island, in Eastern Australia. Taken together, these data suggest that the *A. marina* LARK001 strain is a novel cyanobacterial strain and the first to be isolated from a section of stromatolite where incident light is attenuated and enriched in NIR.

References

1. Manning, W. M. S. H. H., Chlorophyll d: a green pigment in red algae. *J Biol Chem* 1943, *151*, 1-19.
2. HOLT, Further evidence of the relation between 2-desvinyl-2-formyl-chlorophyll a and chlorophyll d. *Can. J. Bot.* **1961,** *39*, 327-331.
3. Holt, A., Further evidence of the relation between 2-desvinyl-2-formyl-chlorophyll a and chlorophyll d. *Can. J. Bot.* **1961,** *39*, 327-331.
4. Miyashita H, I. H., Kurano N, Adachi, K, Chihara M and Miyachi, S., Chlorophyll d as a major pigment. *Nature* **1996,** *383*, 402.
5. Miyashita, H. I., H.; Kurano, N.; Miyachi, S.; Chiharo M., Acaryochloris marina gen. et sp. Nov. (cyanobacteria), an oxygenic photosynthetic prokaryote containing Chl d as a major pigment 1. *J Phycol* **2003,** *2003*, 1247 - 1253.
6. Kuhl, M.; Chen, M.; Ralph, P. J.; Schreiber, U.; Larkum, A. W., Ecology: a niche for cyanobacteria containing chlorophyll d. *Nature* **2005,** *433* (7028), 820.
7. Larkum, A. W.; Kuhl, M., Chlorophyll d: the puzzle resolved. *Trends Plant Sci* **2005,** *10* (8), 355-7.
8. Murakami, A.; Miyashita, H.; Iseki, M.; Adachi, K.; Mimuro, M., Chlorophyll d in an epiphytic cyanobacterium of red algae. *Science* **2004,** *303* (5664), 1633.
9. Miller, S. R.; Augustine, S.; Olson, T. L.; Blankenship, R. E.; Selker, J.; Wood, A. M., Discovery of a free-living chlorophyll d-producing cyanobacterium with a hybrid proteobacterial/cyanobacterial small-subunit rRNA gene. *Proc Natl Acad Sci U S A* **2005,** *102* (3), 850-5.
10. Mohr, R.; Voss, B.; Schliep, M.; Kurz, T.; Maldener, I.; Adams, D. G.; Larkum, A. D.; Chen, M.; Hess, W. R., A new chlorophyll d-containing cyanobacterium: evidence for niche adaptation in the genus Acaryochloris. *ISME J* **2010,** *4* (11), 1456-69.
11. Larkum, A. W.; Chen, M.; Li, Y.; Schliep, M.; Trampe, E.; West, J.; Salih, A.; Kuhl, M., A Novel Epiphytic Chlorophyll d-containing Cyanobacterium Isolated from a Mangrove-associated Red Alga. *J Phycol* **2012,** *48* (6), 1320-7.
12. Behrendt, L.; Larkum, A. W.; Norman, A.; Qvortrup, K.; Chen, M.; Ralph, P.; Sorensen, S. J.; Trampe, E.; Kuhl, M., Endolithic chlorophyll d-containing phototrophs. *ISME J* **2011,** *5* (6), 1072-6.
13. Goh, F.; Allen, M. A.; Leuko, S.; Kawaguchi, T.; Decho, A. W.; Burns, B. P.; Neilan, B. A., Determining the specific microbial populations and their spatial distribution within the stromatolite ecosystem of Shark Bay. *ISME J* **2009,** *3* (4), 383-96.
14. Loughlin, P.; Lin, Y.; Chen, M., Chlorophyll d and Acaryochloris marina: current status. *Photosynth Res* **2013,** *116* (2-3), 277-93.
15. de los Rios, A.; Grube, M.; Sancho, L. G.; Ascaso, C., Ultrastructural and genetic characteristics of endolithic cyanobacterial biofilms colonizing Antarctic granite rocks. *FEMS Microbiol Ecol* **2007,** *59* (2), 386-95.
16. Airs, R. L.; Temperton, B.; Sambles, C.; Farnham, G.; Skill, S. C.; Llewellyn, C. A., Chlorophyll f and chlorophyll d are produced in the cyanobacterium Chlorogloeopsis fritschii when cultured under natural light and near-infrared radiation. *FEBS Lett* **2014,** *588* (20), 3770-7.
17. Averina, S.; Velichko, N.; Senatskaya, E.; Pinevich, A., Far-red light photoadaptations in aquatic cyanobacteria. *Hydrobiologia* **2018,** *813* (1), 1-17.
18. Ho, M. Y.; Bryant, D. A., Global Transcriptional Profiling of the Cyanobacterium Chlorogloeopsis fritschii PCC 9212 in Far-Red Light: Insights Into the Regulation of Chlorophyll d Synthesis. *Front Microbiol* **2019,** *10*, 465.
19. Ho, M. Y.; Shen, G.; Canniffe, D. P.; Zhao, C.; Bryant, D. A., Light-dependent chlorophyll f synthase is a highly divergent paralog of PsbA of photosystem II. *Science* **2016,** *353* (6302).
20. Ho, M. Y.; Soulier, N. T.; Canniffe, D. P.; Shen, G.; Bryant, D. A., Light regulation of pigment and photosystem biosynthesis in cyanobacteria. *Curr Opin Plant Biol* **2017,** *37*, 24-33.
21. Miyashita, H.; Ohkubo, S.; Komatsu, H.; Sorimachi, Y.; Fukayama, D.; Fujinuma, D.; Akutsu, S.; Kobayashi, M., Discovery of chlorophyll d in Acaryochloris marina and chlorophyll f in a unicellular cyanobacterium, strain KC1, isolated from Lake Biwa. *Journal of Physical Chemistry & Biophysics* **2014,** *4* (4), 1.
22. De Los Ríos, A.; Grube, M.; Sancho, L. G.; Ascaso, C., Ultrastructural and genetic characteristics of endolithic cyanobacterial biofilms colonizing Antarctic granite rocks. *FEMS microbiology ecology* **2007,** *59* (2), 386-395.
23. Goh, F.; Allen, M. A.; Leuko, S.; Kawaguchi, T.; Decho, A. W.; Burns, B. P.; Neilan, B. A., Determining the specific microbial populations and their spatial distribution within the stromatolite ecosystem of Shark Bay. *The ISME journal* **2009,** *3* (4), 383-396.
24. Loughlin, P.; Lin, Y.; Chen, M., Chlorophyll d and Acaryochloris marina: current status. *Photosynthesis Research* **2013,** *116* (2), 277-293.

25. McNamara, C. J.; Perry, T. D.; Bearce, K. A.; Hernandez-Duque, G.; Mitchell, R., Epilithic and endolithic bacterial communities in limestone from a Maya archaeological site. *Microbial Ecology* **2006,** *51* (1), 51-64.
26. Partensky, F.; Six, C.; Ratin, M.; Garczarek, L.; Vaulot, D.; Probert, I.; Calteau, A.; Gourvil, P.; Marie, D.; Grebert, T.; Bouchier, C.; Le Panse, S.; Gachenot, M.; Rodriguez, F.; Garrido, J. L., A novel species of the marine cyanobacterium Acaryochloris with a unique pigment content and lifestyle. *Sci Rep* **2018,** *8* (1), 9142.
27. Swingley, W. D.; Chen, M.; Cheung, P. C.; Conrad, A. L.; Dejesa, L. C.; Hao, J.; Honchak, B. M.; Karbach, L. E.; Kurdoglu, A.; Lahiri, S.; Mastrian, S. D.; Miyashita, H.; Page, L.; Ramakrishna, P.; Satoh, S.; Sattley, W. M.; Shimada, Y.; Taylor, H. L.; Tomo, T.; Tsuchiya, T.; Wang, Z. T.; Raymond, J.; Mimuro, M.; Blankenship, R. E.; Touchman, J. W., Niche adaptation and genome expansion in the chlorophyll d-producing cyanobacterium Acaryochloris marina. *Proc Natl Acad Sci U S A* **2008,** *105* (6), 2005-10.
28. Fisher, A.; Wangpraseurt, D.; Larkum, A. W. D.; Johnson, M.; Kuhl, M.; Chen, M.; Wong, H. L.; Burns, B. P., Correlation of bio-optical properties with photosynthetic pigment and microorganism distribution in microbial mats from Hamelin Pool, Australia. *FEMS Microbiol Ecol* **2019,** *95* (1).
29. Ruvindy, R.; White III, R. A.; Neilan, B. A.; Burns, B. P., Unravelling core microbial metabolisms in the hypersaline microbial mats of Shark Bay using high-throughput metagenomics. *The ISME journal* **2016,** *10* (1), 183-196.
30. Wong, H. L.; Smith, D.-L.; Visscher, P. T.; Burns, B. P., Niche differentiation of bacterial communities at a millimeter scale in Shark Bay microbial mats. *Scientific reports* **2015,** *5* (1), 1-17.
31. Wong, H. L.; Visscher, P. T.; White III, R. A.; Smith, D.-L.; Patterson, M. M.; Burns, B. P., Dynamics of archaea at fine spatial scales in Shark Bay mat microbiomes. *Scientific reports* **2017,** *7* (1), 1-12.
32. Wong, H. L.; White, R. A.; Visscher, P. T.; Charlesworth, J. C.; Vázquez-Campos, X.; Burns, B. P., Disentangling the drivers of functional complexity at the metagenomic level in Shark Bay microbial mat microbiomes. *The ISME journal* **2018,** *12* (11), 2619-2639.
33. Schindelin, J.; Arganda-Carreras, I.; Frise, E.; Kaynig, V.; Longair, M.; Pietzsch, T.; Preibisch, S.; Rueden, C.; Saalfeld, S.; Schmid, B.; Tinevez, J. Y.; White, D. J.; Hartenstein, V.; Eliceiri, K.; Tomancak, P.; Cardona, A., Fiji: an open-source platform for biological-image analysis. *Nat Methods* **2012,** *9* (7), 676-82.
34. Herdean, A.; Hall, C. C.; Pham, L. L.; Macdonald Miller, S.; Pernice, M.; Ralph, P. J., Action Spectra and Excitation Emission Matrices reveal the broad range of usable photosynthetic active radiation for Phaeodactylum tricornutum. *Biochim Biophys Acta Bioenerg* **2021,** *1862* (9), 148461.
35. Van Heukelem, L.; Thomas, C. S., Computer-assisted high-performance liquid chromatography method development with applications to the isolation and analysis of phytoplankton pigments. *J Chromatogr A* **2001,** *910* (1), 31-49.
36. Schloss, P. D.; Westcott, S. L.; Ryabin, T.; Hall, J. R.; Hartmann, M.; Hollister, E. B.; Lesniewski, R. A.; Oakley, B. B.; Parks, D. H.; Robinson, C. J.; Sahl, J. W.; Stres, B.; Thallinger, G. G.; Van Horn, D. J.; Weber, C. F., Introducing mothur: open-source, platform-independent, community-supported software for describing and comparing microbial communities. *Appl Environ Microbiol* **2009,** *75* (23), 7537-41.
37. Quast, C.; Pruesse, E.; Yilmaz, P.; Gerken, J.; Schweer, T.; Yarza, P.; Peplies, J.; Glockner, F. O., The SILVA ribosomal RNA gene database project: improved data processing and web-based tools. *Nucleic Acids Res* **2013,** *41* (Database issue), D590-6.
38. Katoh, K.; Standley, D. M., MAFFT multiple sequence alignment software version 7: improvements in performance and usability. *Mol Biol Evol* **2013,** *30* (4), 772-80.
39. Minh, B. Q.; Schmidt, H. A.; Chernomor, O.; Schrempf, D.; Woodhams, M. D.; von Haeseler, A.; Lanfear, R., IQ-TREE 2: New Models and Efficient Methods for Phylogenetic Inference in the Genomic Era. *Mol Biol Evol* **2020,** *37* (5), 1530-1534.
40. Letunic, I.; Bork, P., Interactive Tree Of Life (iTOL) v4: recent updates and new developments. *Nucleic Acids Res* **2019,** *47* (W1), W256-W259.
41. Hill, R.; Schreiber, U.; Gademann, R.; Larkum, A.; Kühl, M.; Ralph, P., Spatial heterogeneity of photosynthesis and the effect of temperature-induced bleaching conditions in three species of corals. *Marine Biology* **2004,** *144* (4), 633-640.
42. Soo, R. M.; Skennerton, C. T.; Sekiguchi, Y.; Imelfort, M.; Paech, S. J.; Dennis, P. G.; Steen, J. A.; Parks, D. H.; Tyson, G. W.; Hugenholtz, P., An expanded genomic representation of the phylum cyanobacteria. *Genome Biol Evol* **2014,** *6* (5), 1031-45.

 doi:10.20944/preprints202204.0112.v1

Appendix A

Supplementary Materials: The following supporting information can be downloaded at: www.mdpi.com/xxx/s1,

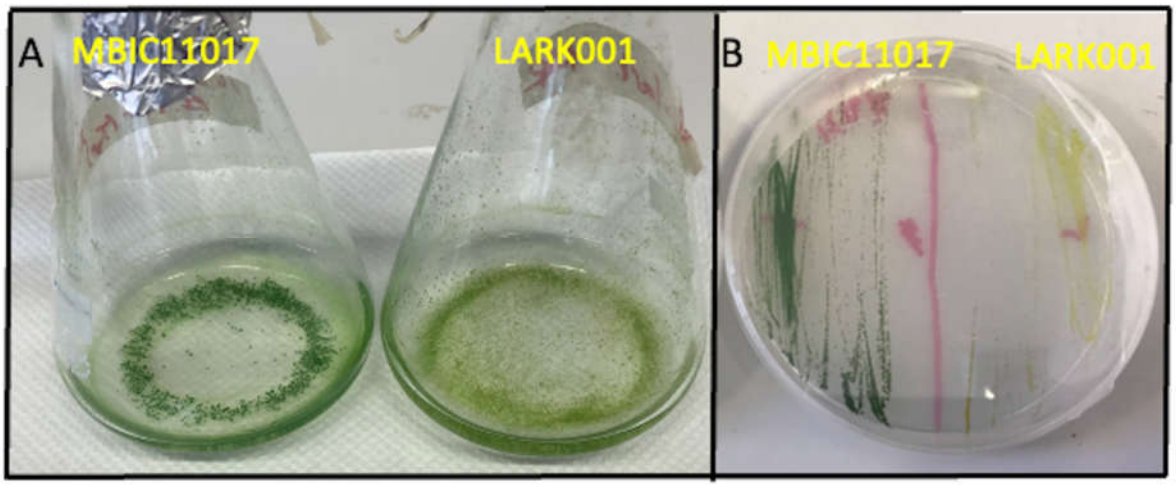

Figure S1. Visual appearance of the cultured strains. Panel A shows the differences in colour and aggregation of each strain when grown in liquid cultures in NIR. Panel B shows similar differences in colour of the strains when grown

Preprints (www.preprints.org) | NOT PEER-REVIEWED | Posted: 12 April 2022 doi:10.20944/preprints202204.0112.v1

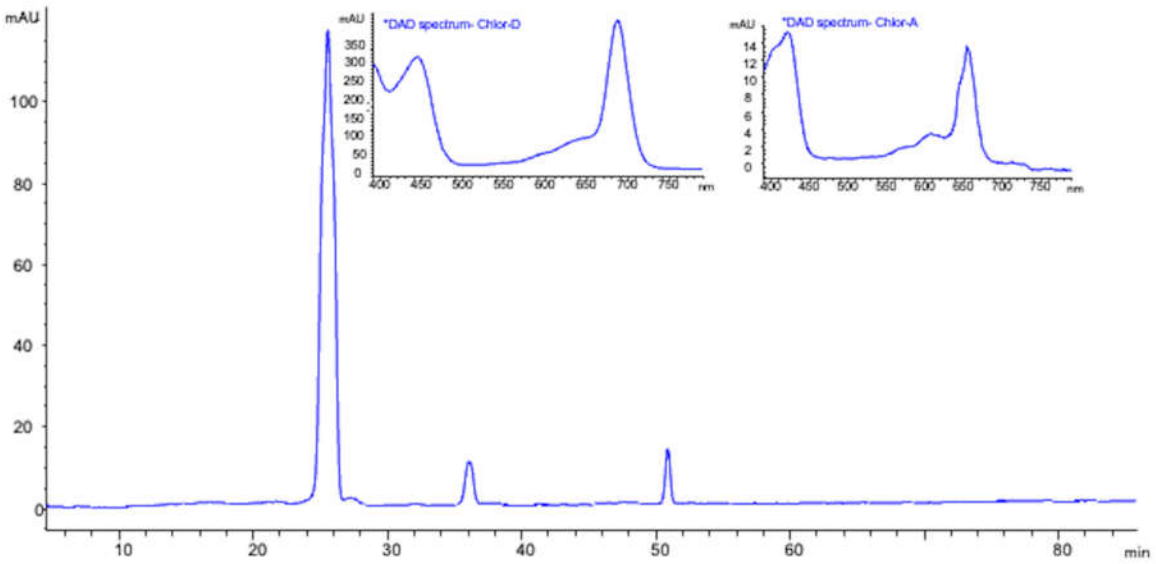

Table S1:

	Chl *a* *mol/L*	Chl *d* *mol/L*	Chl *a*/ Chl *d*	% Chl *d*
Acaryochloris **MBIC11017 (WL)**	0.082	0.857	0.096	91%
Acaryochloris **MBIC11017 (NIR)**	0.032	0.880	0.036	96.4%
Acaryochloris **LARK001 (WL)**	0.052	0.748	0.069	93.4%
Acaryochloris **LARK001 (NIR)**	0.046	0.605	0.076	92.9%

Figure S2. Pigment analysis of the *A. marina* MBIC11017 and LARK0001 strains grown in liquid culture in white light and NIR. The top panel shows a representative HPLC chromatogram showing a major *Chl d* peak at 25.4 minutes retention and a minor Chl *a* peak after 36 minutes retention. Concentration of each peak for each strain at each light condition are summarized in the bottom table.

Author Contributions: For research articles with several authors, a short paragraph specifying their individual contributions must be provided. The following statements should be used "Conceptualization, Michael Johnson and Tony Larkum.; methodology, Michael Johnson (Isolation, Culturing, Fluorescence and Confocal Microscopy), Lisa Sedger (Flow Cytometry), Andrei Herdein (Excitation emission scanning, Fluorometry), Unnikrishnan Kuzhiumparambil (HPLC), Alexander Angelovski (absorbance and fluorescence spectrometry), Brendan Burns (16S rRNA gene sequencing) and Therese Morris (Sampling and sampling permissions); data curation Hon Lun Wong and Gareth Kindler (16S rRNA gene distributions and phylogeny), Michael Johnson (microscopy), Lisa Sedger (Flwo Cytometry); writing—original draft preparation, Michael Johnson and Tony Larkum.; writing—review and editing Michael Johnson, Brendan Burns, Peter Ralph, Lisa Sedger, Andre Herdein, Hon Lun Wong and Tony Larkum. All authors have read and agreed to the published version of the manuscript." Please turn to the CRediT taxonomy for the term explanation. Authorship must be limited to those who have contributed substantially to the work reported.

Funding: This research is supported by the Faculty of Science at UTS.

Data Availability Statement: All primary data is stored as a digital resource at UTS and is available upon request to the corresponding author**.** DNA sequence has been uploaded as fastq sequences to MG-RAST (https://www.mg-rast.org/mgmain.html?mgpage=project&project=mgp100232)

Acknowledgments: The authors thank Mrs Sarah Osvath for general laboratory support and Mr Zhongran Ni for initial advice on gDNA extraction.

Conflicts of Interest: The authors declare no conflict of interest.

 doi:10.20944/preprints202204.0112.v1